TROPOMI validation report of the Aerosol Optical Thickness product

document number	:	S5P-KNMI-L2-0402-RP
authors	:	M. de Graaf
CI identification	:	*None*
issue	:	1.0.0
date	:	2022-02-10
status	:	released

Document approval record

	digital signature
Prepared:	Martin de Graaf Digitally signed by Martin de Graaf Date: 2022.02.10 11:19:29 +01'00'
Checked:	
Approved PM:	
Approved PI:	

Document change record

issue	date	item	comments
0.0.1	2020-08-11	All	Initial version
0.0.2	2020-09-24	All	Version shared with team (confidential)
0.0.3	2020-11-26		Corrections after review:
		Ch. 6	-Update of validation strategy
		Ch. 7	-Update of validation results
1.0.0	2021-06-01	All	Public release

Contents

List of Tables

List of Figures

1 Introduction

1.1 Identification

This document is identified as S5P-KNMI-L2-0402-RP.

1.2 Purpose and objective

This document is the Validation Report (VR) of the Aerosol Optical Thickness (AOT) product derived from observations made by the TROPOMI instrument on the Sentinel-5 Precursor satellite. The purpose of this VR is to present the validation approach, to present the results from the validation, and to report to the users the quality that they may expect. The document is maintained during the development phase of the data product in the context of the S5p+I project. Two updates of the document are planned.

1.3 Document overview

The structure of this VR is as follows. In section 2 applicable, standard and reference documents are listed. Section 3 introduces terms and definitions used in this VR, along with a list of acronyms and abbreviations that are used throughout the VR. Section 4 provides a reference to a general description of the TROPOMI instrument. Section 5 introduces the AOT algorithm approach, the heritage involved, and the requirements appropriate to the product and the validation. The validation strategy is outlined in section 6. Next, the validation results are presented in section 7. This VR ends with a summary of the validation results in section 8.

2 Applicable and reference documents

2.1 Applicable documents

[AD1] TROPOMI Instrument and Performance Overview.
source: KNMI; **ref:** S5P-KNMI-L2-0010-RP; **issue:** 0.10.0; **date:** 2014-03-15.

[AD2] TROPOMI ATBD of the Aerosol Optical Thickness.
source: KNMI; **ref:** S5P-KNMI-L2-0033-RP; **issue:** 1.0.0; **date:** 2021-06-01.

2.2 Standard documents

[SD1] Space Engineering – Software.
source: ESA/ECSS; **ref:** ECSS-E-ST-40C; **date:** 2009-03-06.

2.3 Reference documents

[RD1] Terms, definitions and abbreviations for TROPOMI L01b data processor.
source: KNMI; **ref:** S5P-KNMI-L01B-0004-LI; **issue:** 3.0.0; **date:** 2013-11-08.

[RD2] Terms and symbols in the TROPOMI Algorithm Team.
source: KNMI; **ref:** S5P-KNMI-L2-0049-MA; **issue:** 1.0.0; **date:** 2015-07-16.

[RD3] H. Jethva and O. Torres; Satellite-based evidence of wavelength-dependent aerosol absorption in biomass burning smoke inferred from Ozone Monitoring Instrument. *Atmos. Chem. Phys.*; **11** (2011), 10541; 10.5194/acp-11-10541-2011.

[RD4] B. T. Johnson, K. P. Shine and P. M. Forster; The semi–direct aerosol effect: Impact of absorbing aerosols on marine stratocumulus. *Quart. J. Roy. Meteor. Soc.*; **130** (2004), 1407; 10.1256/qj.03.61.

[RD5] M. de Graaf, N. Bellouin, L. G. Tilstra *et al.*; Aerosol direct radiative effect of smoke over clouds over the southeast Atlantic Ocean from 2006 to 2009. *Geophys. Res. Lett.*; (2014); 10.1002/2014GL061103. URL `http://dx.doi.org/10.1002/2014GL061103`.

[RD6] Omar Torres, Hiren Jethva and P. K. Bhartia; Retrieval of Aerosol Optical Depth above Clouds from OMI Observations: Sensitivity Analysis and Case Studies. *J. Atmos. Sci.*; **69** (2011) (3), 0022–4928; 10.1175/JAS-D-11-0130.1.

[RD7] Hiren Jethva, Omar Torres, Fabien Waquet *et al.*; How do A-train Sensors Intercompare in the Retrieval of Above-Cloud Aerosol Optical Depth? A Case Study-based Assessment. *Geophys. Res. Lett.*; **41** (2014); 10.1002/2013GL058405.

[RD8] F. Peers, P. Francis, C. Fox *et al.*; Observation of absorbing aerosols above clouds over the south-east Atlantic Ocean from the geostationary satellite SEVIRI – Part 1: Method description and sensitivity. *Atmos. Chem. Phys.*; **19** (2019) (14), 9595; 10.5194/acp-19-9595-2019.

[RD9] O. Dubovik, M. Herman, A. Holdak *et al.*; Statistically optimized inversion algorithm for enhanced retrieval of aerosol properties from spectral multi-angle polarimetric satellite observations. *Atmospheric Measurement Techniques*; **4** (2011) (5), 975; 10.5194/amt-4-975-2011.

[RD10] TROPOMI validation report:GRASP BRDF + AOD.
source: Grasp; **ref:** S5P- - -; **issue:** 0.0.1; **date:** 2020-09-25.

[RD11] A. A. Kokhanovsky, J. L. Deuzé, D. J. Diner *et al.*; The inter-comparison of major satellite aerosol retrieval algorithms using simulated intensity and polarization characteristics of reflected light. *Atmospheric Measurement Techniques*; **3** (2010) (4), 909; 10.5194/amt-3-909-2010. URL `https://www.atmos-meas-tech.net/3/909/2010/`.

[RD12] Yerong Wu, Martin de Graaf and Massimo Menenti; The Sensitivity of AOD Retrieval to Aerosol Type and Vertical Distribution over Land with MODIS Data. *Remote Sensing*; **8** (2016) (9); 10.3390/rs8090765. URL `http://www.mdpi.com/2072-4292/8/9/765`.

[RD13] ESA Climate Change Initiative, Option 3 Absorbing Aerosol Round Robin.
source: ESA; **ref:** Aerosol Absorption; **issue:** 1.2; **date:** 2018-03-15.

[RD14] Nick Schutgens, Oleg Dubovik, Otto Hasekamp *et al.*; AEROCOM and AEROSAT AAOD and SSA study - Part 1: Evaluation and intercomparison of satellite measurements. *Atmospheric Chemistry and Physics*; **21** (2021) (9), 6895; 10.5194/acp-21-6895-2021.

2.4 Electronic references

[ER1] URL `https://aeronet.gsfc.nasa.gov/`.

3 Terms, definitions and abbreviated terms

Terms, definitions and abbreviated terms that are used in the documentation of the TROPOMI L0-1b data processor are described in [RD1]. Terms, definitions and abbreviated terms for TROPOMI Level 2 algorithms are described in [RD2]. Terms, definitions and abbreviated terms specific for this document are defined below.

3.1 Terms and definitions

There are no document specific terms and definitions.

3.2 Acronyms and abbreviations

AAI	Absorbing Aerosol Index
AAOT	Aerosol Absorption Optical Thickness
AOD	Aerosol Optical (Penetration) Depth
AOT	Aerosol Optical Thickness (partial - layer, or total - atmosphere)
ATBD	Algorithm Theoretical Baseline Document
BRDF	Bidirectional Reflectance Distribution Function
BSA	Black-Sky Albedo
CAMS	Copernicus Atmosphere Monitoring Service
CF	Climate and Forecast metadata conventions
DAK	Doubling-Adding KNMI
DU	Dobson Units, 2.69$\times$10^{16} molecules cm^{-2}
ECMWF	European Centre for Medium-Range Weather Forecast
ENVISAT	Environmental Satellite
EOS-Aura	Earth Observing System – Aura satellite
EPS-SG	EUMETSAT Polar System – Second Generation
ERS	European Remote Sensing Satellite
ESA	European Space Agency
EUMETSAT	European Organisation for the Exploitation of Meteorological Satellites
FOV	Field-of-View
FRESCO	Fast Retrieval Scheme for Clouds from the Oxygen A band
GMTED2010	Global Multi-resolution Terrain Elevation Data 2010
GOME	Global Ozone Monitoring Experiment
HDF	Hierarchical Data Format
KNMI	Koninklijk Nederlands Meteorologisch Instituut
LER	Lambertian-Equivalent Reflectivity
LUT	Look-Up Table
L2OP	Level-2 Operational Processor
L2PP	Level-2 Prototype Processor
MERIS	Medium Resolution Imaging Spectrometer
METOP	Meteorological Operational Satellite
MLS	Mid-Latitude Summer
NASA	National Aeronautics and Space Administration
NISE	Near-real-time Ice and Snow Extent
NRT	Near-Real-Time
OMI	Ozone Monitoring Instrument
PAL	Product Algorithm Laboratory
PAM	Performance Assessment Module

RAA	Relative Azimuth Angle
RMSE	Root-Mean-Square Error
RTM	Radiative Transfer Model
SAA	Solar Azimuth Angle
SCIAMACHY	Scanning Imaging Absorption Spectrometer for Atmospheric Chartography
SW	Software
SZA	Solar Zenith Angle
S5	Sentinel-5 mission
S5P	Sentinel-5 Precursor mission
Suomi-NPP	Suomi-National Polar-Orbiting Partnership
TOA	Top-of-Atmosphere
TOMS	Total Ozone Mapping Spectrometer
TROPOMI	Tropospheric Monitoring Instrument
UTC	Coordinated Universal Time
UV	Ultraviolet
UVNS	Ultraviolet Visible Near-infrared Shortwave spectrometer
VAA	Viewing Azimuth Angle
VIS	Visible
VZA	Viewing Zenith Angle

4 TROPOMI instrument description

A description of the TROPOMI instrument and performance can be found in [AD1].

5 Introduction to the TROPOMI AOT product

Aerosol particles scatter and absorb light, thus affecting the radiation field in the atmosphere. On the short-term, this may have impact on weather, and over longer term on climate. In addition to direct radiative effects due to scattering and absorption, aerosols also impact the formation, the droplet size, the albedo, precipitation and lifetimes of clouds. These aerosol-cloud interactions thus also impact weather and climate. Aerosol also have adverse health effects. Especially small aerosol particles can penetrate deep into the respiration system, causing short-term and long-term health risks.

- A common classification for aerosol is according to their sources. Aerosol particles which are emitted as particles, such as desert dust, volcanic ash or sea salt, are referred to as primary aerosols. Secondary aerosols are formed within the atmosphere from precursor gases, such as sulphur dioxide, nitrogen dioxide, organics and ammonia. Due to their different formation process, primary aerosol particles are generally larger than secondary aerosol particles.
- Another way of classifying aerosol particles is according to their absorption. The amount of absorption is commonly expressed as the single scattering albedo, which is defined as the ratio between scattering and extinction. The single scattering albedo of atmospheric aerosols varies in the range between approximately 0.7 and 1.0. Absorbing components in aerosol particles that determine the amount of absorption include iron oxides in desert dust and volcanic plumes, and black and brown carbon for plumes resulting from (incomplete) combustion processes.
- A third classification of aerosol particles is according to their hygroscopic behaviour. Aerosol particles that contain a significant amount of chemical components such as sea salt, ammonium sulphate and ammonium nitrate, as well as sulphuric acid, that will attract water when the relative humidity increases and are called hygroscopic. Particles that do not attract water are called hydrophobic. Hygroscopic particles will significantly change size and composition with changing relative humidity, which also impacts their scattering and absorbing properties.
- Aerosol particles can also be classified according to their shape. Primary particles that are hydrophobic, such as desert dust and volcanic ash, are generally non-spherical. Secondary aerosols and hygroscopic particles are generally spherical.

The algorithm described in this document is designed to retrieve the aerosol optical thickness (AOT) in the wavelength range between 340 and 494 nm. This wavelength range is selected because it contains unique information on absorption by aerosols. The high-spectral information from UVNS spectrometers like TROPOMI are important to derive the spectral variation in aerosol absorption, and should be exploited as such. There are indications that the absorption by aerosols in the UV may be much larger than previously anticipated [RD3], and the UV-absorption has important consequences for the formation and life-time of clouds [RD4, RD5]. A detailed description can be found in [AD2].

It is expected the 3MI instrument on Metop Second Generation, which is designed to derive aerosol properties, will provide the AOT in the visible and near infrared with a higher trueness and spatial resolution than what can be achieved from the UVNS instrument.

5.1 Heritage

Satellite observations in the wavelength region from approximately 340 to 400 nm are sensitive to the presence of elevated absorbing aerosols. The UV Aerosol Index (UV-AI, also called absorbing aerosol index or AAI) has been derived from almost all ozone monitoring instruments such as TOMS, GOME-1, SCIAMACHY, OMI and GOME-2. Although the UV-AI is widely used, it also has its limitations. The main limitation is that the UV-AI is not a geophysical quantity, as such it cannot be compared to models or observations using other techniques. Therefore, this ATBD focuses on the AOT and the absorbing part of the AOT (AAOT). The AOT and AAOT can only be derived for cloud-free pixels, because the algorithm cannot distinguish between clouds and aerosols. This is a strong limitation of this product. In addition, it is not possible to derive AOT and AAOT over strongly reflecting surfaces such as snow or ice. Note that the retrieval of AOT and AAOT over clouds is a field of active research [RD6, RD5, RD7, RD8].

Cloud contamination is one of the largest challenges for AOT retrievals from satellite observations. The number of cloud-free pixels depends strongly on the spatial resolution of the observations. Therefore, satellite instruments designed to detect aerosols, such as MODIS, MISR and 3MI, have a relatively good spatial resolution and a relatively low spectral resolution. The 340 to 400 nm range has traditionally been observed by satellite instruments designed to measure trace gases, which have a high spectral resolution but a low spatial resolution. OMI with 13x24 km^2 had the best spatial resolution in the targeted wavelength region. For OMI, two AOT products were developed: the OMAERO algorithm that uses 14 wavelengths in the range 354 – 500 nm, and the OMAERUV algorithm that is based on the retrieval at 354 and 388 nm (Torres et al., 2002, 2007, 2013). The OMAERUV algorithm is especially targeting the wavelength range that is also the main target for this ATBD and has been designed to derive both the AOT and AAOT. Both the OMAERO and the OMAERUV algorithms are using a look-up table (LUT) approach. The algorithm described in this ATBD for S5P/TROPOMI combines these approaches.

The combination of AOT and AAOT is especially important to distinguish different aerosol types, e.g. desert dust, biomass burning and weakly absorbing particles. In addition, it is directly related to the absorption of solar radiation in aerosol layers, which affect the radiation balance and vertical stability of the atmosphere, and modify the formation processes and the lifetime of clouds.

In addition to the specialized TROPOMI algorithm, a generalized aerosol retrieval algorithm GRASP is being developed in parallel [RD9]. The GRASP algorithm can handle the UV wavelength range and can be setup to derive the AOT and AAOT. GRASP is an iterative scheme, that is based on on-line radiative transfer.

AOT at visible and NIR wavelength are also available, e.g. from the specialised instruments like MODIS, MISR and 3MI. An effective AOT at 760 nm is available from the S5P ALH algorithm, which fits the reflectance spectrum in the O_2-A band in the NIR wavelength band. However, the aerosol model for this fit is a very simple one.

5.2 Requirements

These are the GCOS climate application requirements for AOT:

- The uncertainty in the aerosol optical thickness (AOT) for two or more wavelengths in the spectral region between 340 nm and 390 nm shall be smaller than 0.05 (target) to 0.10 (threshold) or 10% (target) to 25% (threshold). Depending on the scenario the least stringent of the absolute and the relative requirements applies.
- The uncertainty in the aerosol optical thickness (AOT) for one or more wavelengths in the spectral region between 390 nm and 500 nm shall be smaller than 0.02 (target) to 0.10 (threshold) or 10(target) to 25% (threshold). Depending on the scenario the least stringent of the absolute and the relative requirements applies.

The S5P-TROPOMI AOT and AAOT at the UV wavelengths are not expected to meet these requirements. Based on the experience with the OMAERUV algorithm and expected improvements of the algorithm and the instrument, an accuracy of 0.1 or 25% (whichever is largest) is expected for near-global, operational performance (solar zenith angles less than 70°). Larger errors are expected for high solar zenith angles. At higher solar zenith angles the problems with cloud clearing will increase due to the longer path through the atmosphere. Also, the representation errors between the satellite and the ground-based observation will increase. Furthermore, uncertainties in the radiative transfer will become larger. Therefore the performance range to solar zenith angles is limited to less than 70°. At higher solar zenith angles the data will be flagged as having lower quality.

6 Validation strategy

The validation approach consists of comparisons with ground-based observations by the AErosol RObotic NETwork (AERONET) [ER1] and VIIRS AOD product. The results from the validation study are presented in section 7.

For the ground-based observations, in total 32 AERONET stations were studied for the ground-based validation, see section 7.1. Two stations in Italy, Lecce and Ispra, and thirty more stations at widely varying locations were studied to include all relevant aerosol types found around the globe. The locations of these stations are indicated in Fig 10. These are the same AERONET stations that were selected for the validation of the GRASP BRDF and AOD product (see [RD10]). The stations marked in red did not have valid data at the moment of writing for the month March and April 2021.

AERONET data can be downloaded freely, are widely used, and are considered to be a reliable reference by the aerosol community. Because AERONET stations perform their measurements multiple times per hour, finding suitable collocations with the TROPOMI observations is straightforward. The latest version of AERONET data (3.0), Level 1.5 (Cloud-screened and quality controlled) were used. In section 7.1.1 a detailed analysis of the TROPOMI AOT and SSA is presented for three months (January – March) in 2019 and 2020 near the AERONET stations Lecce and Ispra in Italy. The Po region in Italy suffered an early and strict lock-down due to Covid-19 infections in the spring of 2020, and the data were collected and processed to study changes in aerosol concentrations due to the lock-down measures, which provided a unique opportunity to study the accuracy of the TROPOMI UV AOT product.

In section 7.1.2 the global characteristics of the AOT product are presented using a comparision with globally distributed AERONET stations, using a more statistical analysis.

Furthermore, in section 7.2 the product is compared to AOT from a different instrument: VIIRS onboard Suomi-NPP. This instrument flies in synchrony with Sentinel-5 Presursor and is ideal for collocating measurements.

7 Validation results

7.1 Comparison with AERONET data

The validation approach consists of comparisons with ground-based observations by the Aerosol Robotic Network (AERONET) [ER1]. The AERONET data are considered to be a reliable reference for aerosol properties (AOT and SSA) and often used for validation studies.

In the following, AERONET data are compared to TROPOMI data within a radius of 200 km of the station. The TROPOMI data are compared to the closest (in time) AERONET measurement, which are available about every 15 minutes. TROPOMI AOT measurements are always between 0 and 10 due to LUT limits, no filters were applied.

7.1.1 Italy and Po region

The Sentinel-5P/TROPOMI AOT and SSA were retrieved over an area between 35 – 46°N and 7 – 20 °E during January – March 2019 and 2020. For these two periods the AOT is expected to vary considerably during the two years, However, an extensive study using TROPOMI and GRASP AOT data showed no systematic changes between the two years when comparing the AOT during the two years in spite of the stringent Covid-19 measures that were in effect in the year 2020. The effect of the Covid-19 measures on aerosols are likely more prominent in the type of aerosols than in the amount, but this needs additional research.

An example of the retrieval of the AOT and SSA at 380 nm by TROPOMI on 7 January 2019 is shown in Fig. 1. The AOT is typically low, in the order of 0.2, but in the Po valley the values are significantly higher. This may be due to industrial activities and traffic.

The results from these two years were used to perform a first verification of the AOT using AERONET measurements. Two AERONET stations were selected, which produced AOT measurements almost constantly during both periods, and cover two different parts of the selected area:

1. University of Lecce (40°20’N ; 18°6’E, 30 m altitude)
2. Ispra (45°48’N ; 8°37’E, 235 m altitude)

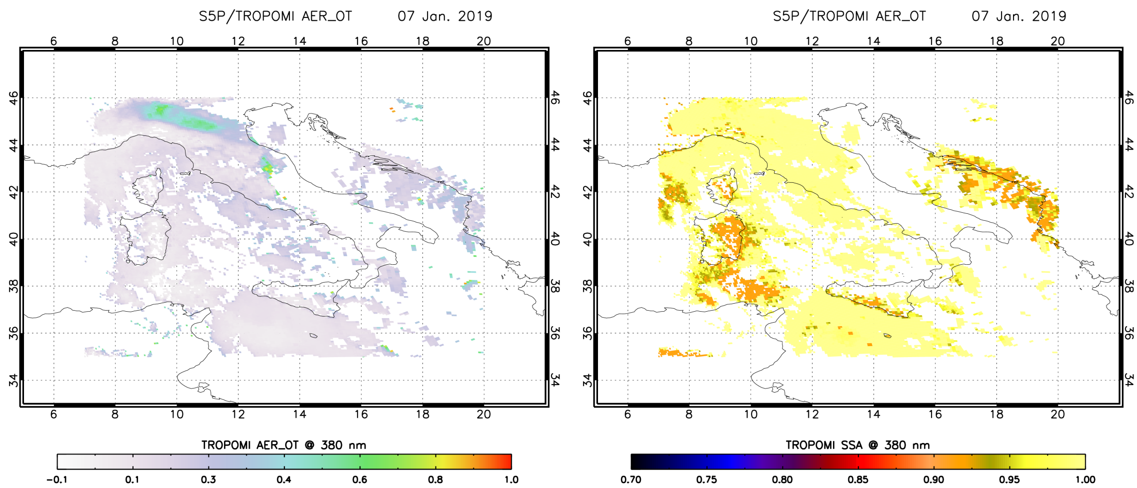

Figure 1: AOT and SSA at 380 nm on 7 January 2019, retrieved from Sentinel-5P/TROPOMI over the Po area and the Mediterranean around Italy.

7.1.1.1 Case 1: Lecce (2019)

The first AERONET station is the University of Lecce, in the south-east corner of the considered area, at an altitude of 30 m. This station is near the Mediterranean Sea, and prone to excursions of dust from the nearby Sahara, smoke from vegetation fires in the dry countries surrounding the Mediterranean Sea, and occasionally volcanic ash from the nearby volcanoes like Etna and others, making it a very interesting station to study

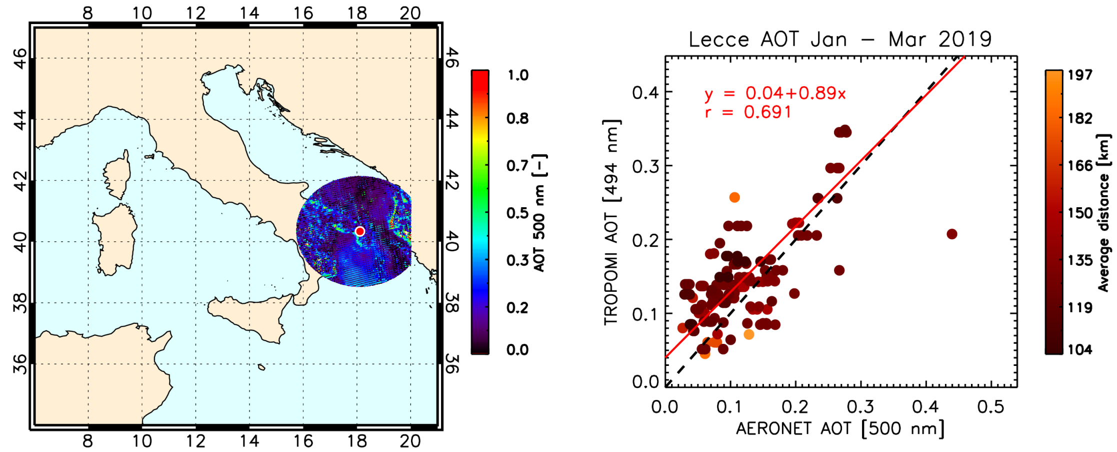

Figure 2: (left) S5P AOT (each measurement is overplotted) retrieved around the University of Lecce, showing the 200 km radius within which the average AOT during Jan – Mar 2019 is compared with collocated (in time) AERONET AOT; (right) Scatterplot of the S5P AOT at 494 nm compared to AERONET AOT at 500 nm. For each AERONET measurement (roughly every 15 minutes) the S5P AOT measurements within these 15 minutes closer than 200 km to the station were averaged, weighted by distance to the station. The average distance to the station for each measurement average is indicated by the color of the dot. The dashed line indicates the 1–1 line, the red line is the linear least squares fit, weighted by the distance of each TROPOMI measurement to the AERONET station, given by *y*. *r* is Pearson's correlation coeffient.

absorbing aerosols. Here, we focus on the continuous AOT measurements, which are generally low, in the order of 0.1–0.2, with occasional peaks during plume overpasses.

Figure 2 shows the location of the station, the radius of 200 km around the station within which TROPOMI measurements are considered, and a comparison between the AERONET AOT measurements and the TROPOMI AOT measurements. The AERONET AOT at 500 nm is considered, while for TROPOMI the largest wavelength of 494 nm is considered. All collocated measurements between 1 January 2019 and 31 March 2019 were compared. For each AERONET AOT measurement the TROPOMI measurements closest (in time) to that AERONET measurement were averaged if these measurements were closer than 200 km to the station.

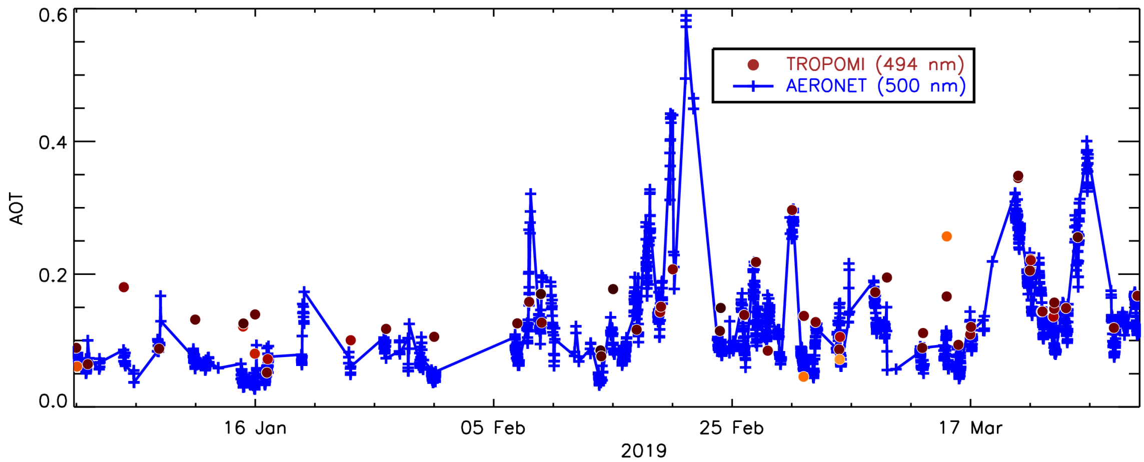

Figure 3: Temporal AOT at 500 nm at the University of Lecce AERONET station between 1 January and 31 March 2019 (blue), compared to the average S5P AOT at 494 nm (brown). The dots correspond to the dots in the scatterplot of Fig. 2, with the same colorscale and interpretation. They are the weighted (by distance) averages of all S5P measurements within 15 min of an AERONET measurement and within 200 km of the station.

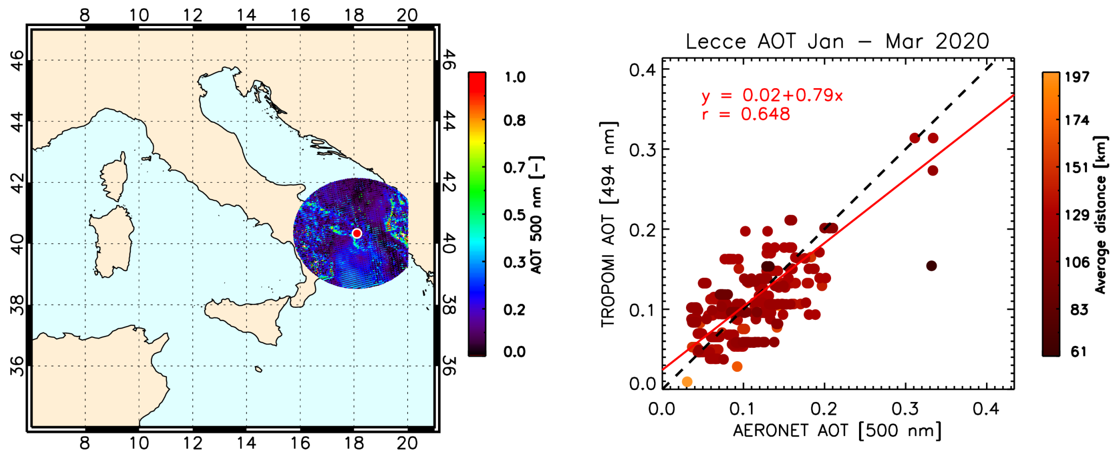

Figure 4: Same as Fig. 4, but for 2020.

AERONET reports roughly one measurement per 15 minutes, so only TROPOMI measurements within these 15 minutes were averaged, and the average was weighted to the individual distance of each measurement to the station. The scatterplot shows a very good comparison between the two measurements, which is in line with the accuracy of AOT derived single-view satellite instruments. The difference between the TROPOMI and AERONET AOT is never more than about 0.1.

Figure 3 shows the temporal development of the AOT at 500 nm for Lecce in blue, and the collocated, averaged AOT at 494 nm from TROPOMI in brown. The brown dots correspond to the dots in the scatterplot in Fig. 2. Clearly, the behaviour of the AOT from AERONET and TROPOMI show a high correspondence, in line with the scatterplot in Fig. 2. This means that the measurements are sensitive to the same (aerosol) signals.

7.1.1.2 Lecce (2020)

To investigate the Covid-19 measures on the development on AOT, the AOT was retrieved from TROPOMI measurements in 2020 as well. These measurements were compared to AERONET measurements at Lecce University in the same way as in 2019, see Figure 4 and 5.

The figures show that the correlation between the TROPOMI AOT at 494 nm and AERONET AOT at 500 nm is as strong as in 2019. However, in general the AOT in 2020 is higher than in 2019, and in general there seem to be more frequent incursions of smoke or dust in 2020, increasing the AOT. Although the TROPOMI AOT is similarly sensitive to these measurements as AERONET, confirming the accuracy of the retrieval, this is

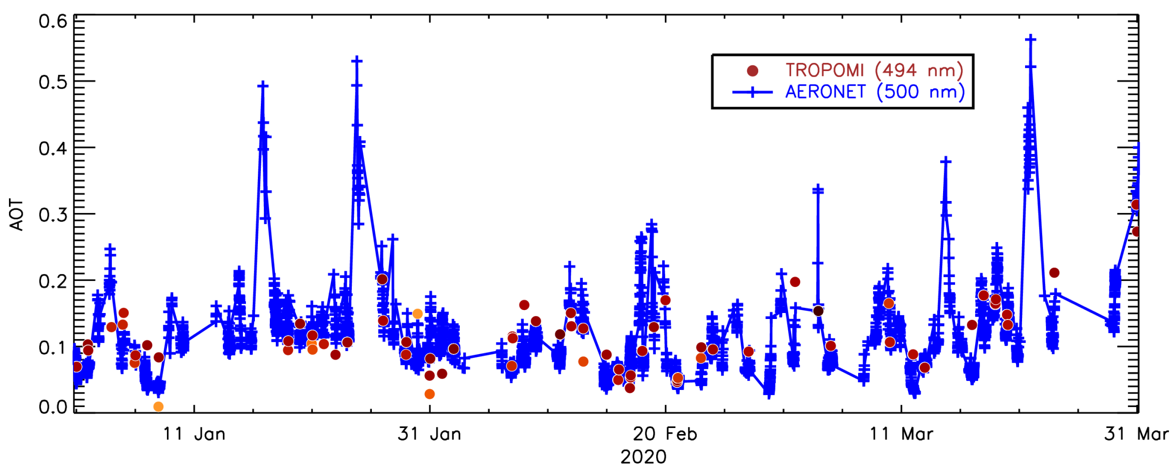

Figure 5: Same as Fig. 3, but for 2020.

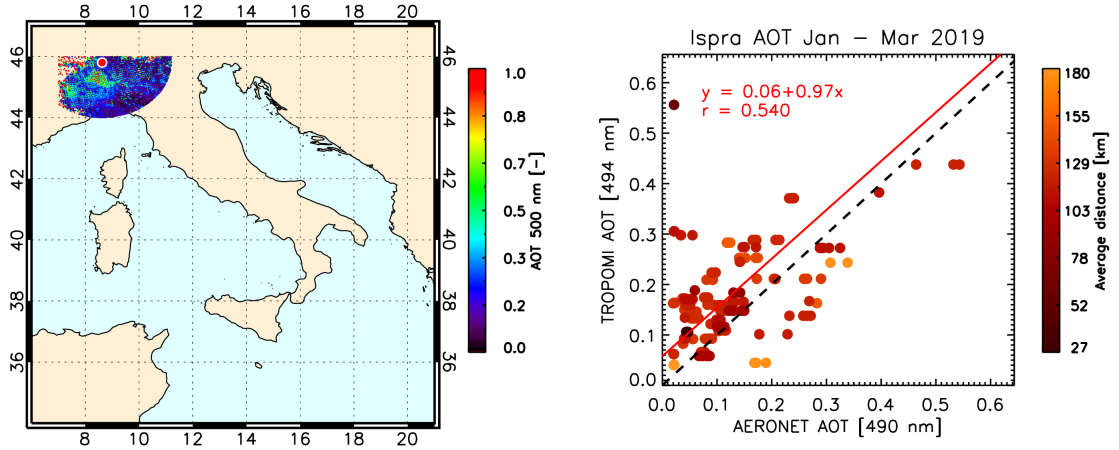

Figure 6: (left) S5P AOT (each measurement is overplotted) retrieved around Ispra, showing the 200 km radius within which the average AOT during Jan – Mar 2019 is compared with collocated (in time) AERONET AOT. The station is located at the very northern edge of the research area, therefore only measurements south of the station were considered. (right) Scatterplot of the S5P AOT at 494 nm compared to AERONET AOT at 490 nm. For each AERONET measurement (roughly every 15 minutes) the S5P AOT measurements within these 15 minutes closer than 200 km to the station were averaged, weighted by distance to the station. The average distance to the station for each measurement average is indicated by the color of the dot. The dashed line indicates the 1–1 line, the red line is the linear least squares fit, weighted by the distance of each TROPOMI measurement to the AERONET station, given by *y*. *r* is Pearson's correlation coeffient.

disadvantageous for the Covid-19 measures research, which will have to focus on the background signal of the AOT during quiet days without external dust and smoke. However, for the purpose of verification, which is the focus here, the measurements nicely confirm the accuracy of the TROPOMI AOT retrieval.

7.1.1.3 Case 2: Ispra (2019)

Next, the verification was repeated using the measurements from the AERONET station Ispra at (45°48'N; 8°37'E). This station is located at the North-west of the Po valley at an altitude of 235 m. It produced near-continuous measurements in the first quarter of 2019 and 2020, except for a large gap in January 2019. However, from all AERONET stations in the northern part of the research area and near the Po valley, this

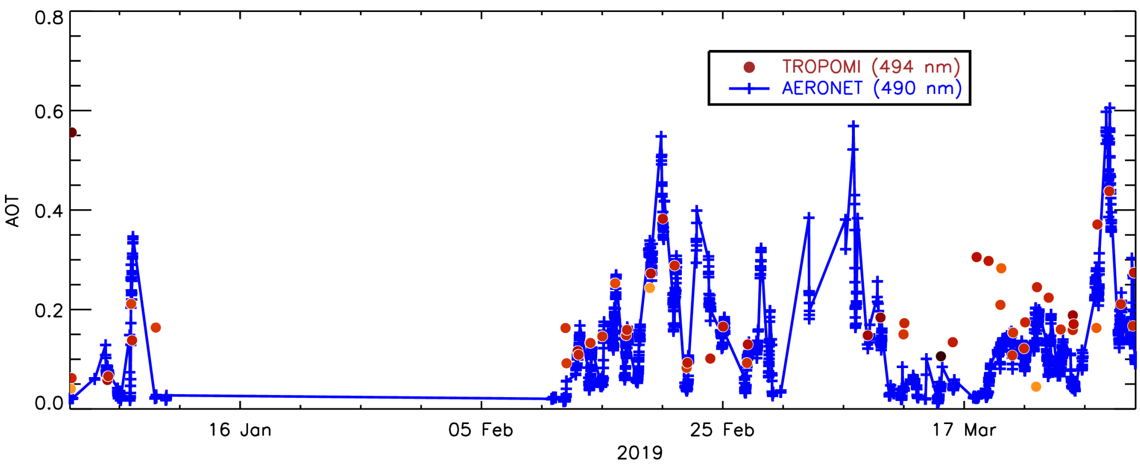

Figure 7: Temporal AOT at 490 nm at the Ispra AERONET station between 1 January and 31 March 2019 (blue), compared to the average S5P AOT at 494 nm (brown). The brown dots correspond to the dots in the scatterplot of Fig. 6, with the same colorscale and interpretation. They are the weighted (to distance) averages of all S5P measurements within 15 min of the AERONET measurement and within 200 km of the station.

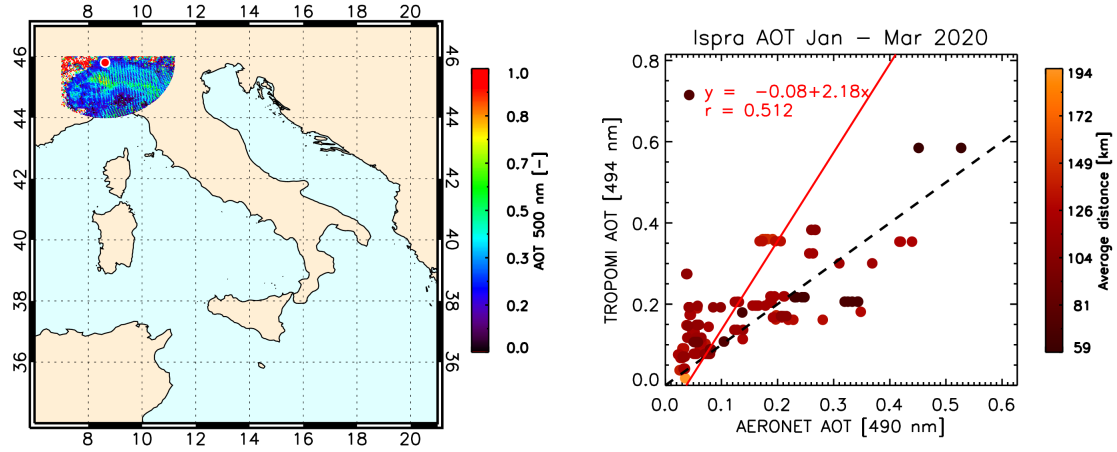

Figure 8: Same as Fig. 8, but for 2020.

station had the best temporal coverage. The AOT measurements for this station are reported at 490 nm.

Figures 6 and 7 show a similar correspondence between the TROPOMI and AERONET AOT measurements, with perhaps a few more outliers. It has to be noticed that Ispra is located in an mountainous area near the Alps, although most measurements were located over the Po valley. In general, the AOT measurements over land are less reliable than over the dark surface of the sea, so a lower accuracy is not surprising.

7.1.1.4 Case 2: Ispra (2020)

The results for Ispra in 2020 are presented in Fig 8 and Fig 9.

In general, a lower baseline AOT in 2020 than in 2019, which might be expected from the Covid-19 measures in 2020, cannot be judged from Figs. 7 and 9. Unfortunately, in 2019 the AERONET measurements are missing for a large part in January, while in February and March 2019 fairly high AOT values are measured. It is unclear whether this is common industrial AOT for the Po valley, or incursions from dust and smoke from around. Variations are fairly large.

In 2020 the AOT is also variable, and generally as large as in 2019. However, due to the missing AERONET measurements this is difficult to judge here. A study of TROPOMI AOT over dedicated areas may shed more light on this issue. Here, it can be concluded that the accuracy of TROPOMI AOT is well within expectations.

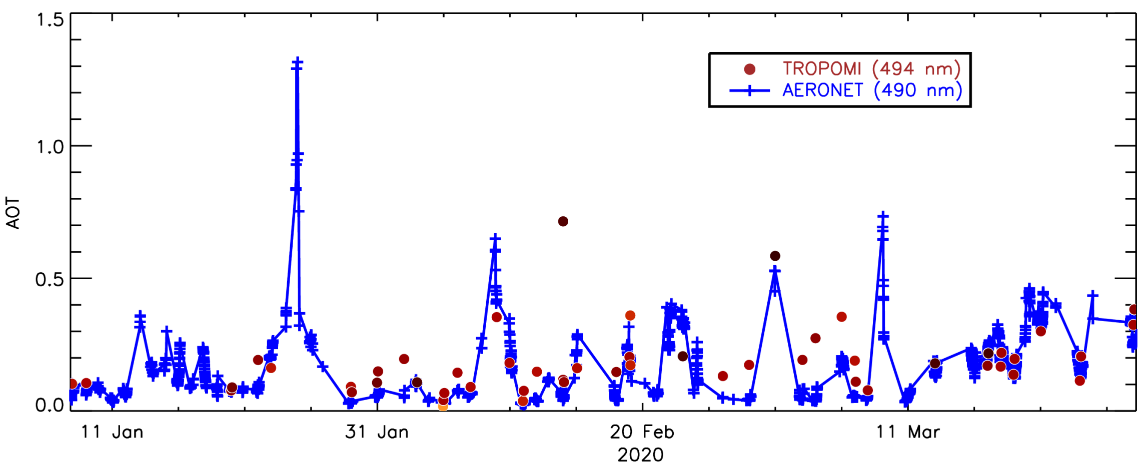

Figure 9: Same as Fig. 7, but for 2020.

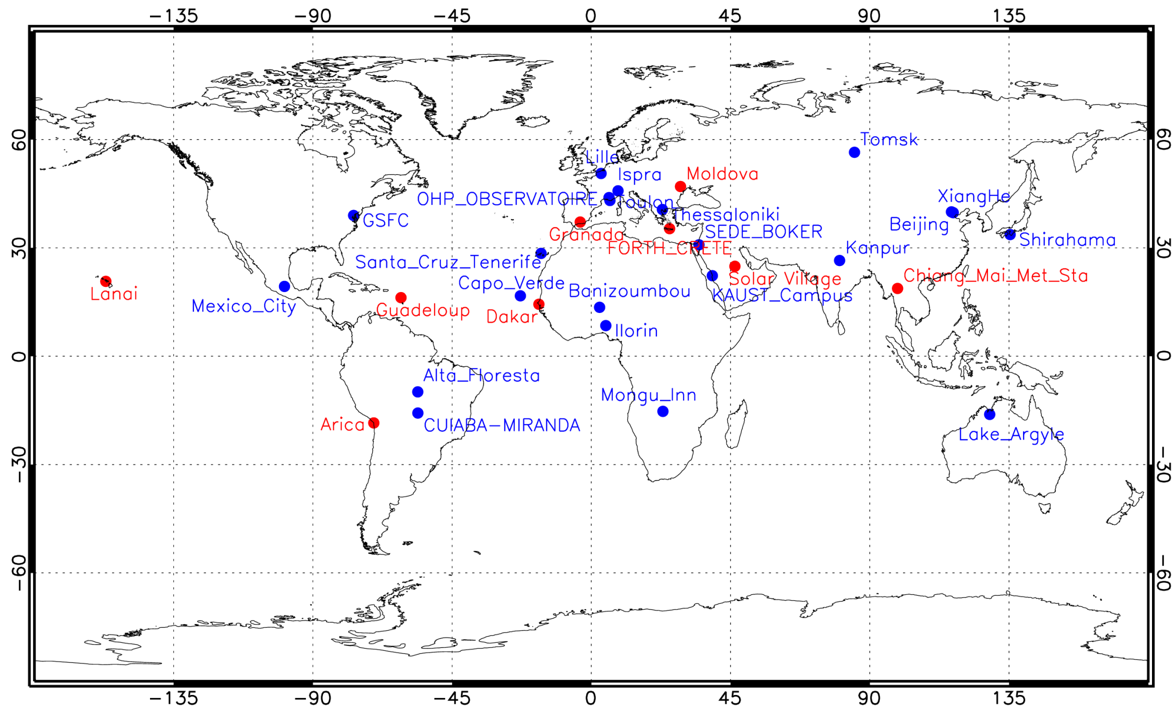

Figure 10: Global distribution of the 32 selected AERONET stations. The station marked in red did not have any (V1.5) data during March and April 2021.

7.1.2 Global AERONET data

After the developement of the scientific AOT algorithm, the processor was ported to the Product Algorithm Laboratory (PAL), newly developed by ESA. There, the AOT was processed for the year 2019 and for two months in 2021 (March and April). The latest data in 2021 was used to validate the aerosol optical thickness product against a global set of AERONET data. Thirty stations were selected for comparisons, as shown in Figure 10. Of these stations, six station produced no data during the selected months, and 3 more stations only delivered level 1.0 data. These statsion are marked red in Figure 10. For the 21 remaining stations the version 3, Level 1.5 AERONET AOT at 500 nm was compared to the AOT at 494 nm from TROPOMI, using all measurements within 15 minutes of an AERONET measurement, within 200 km of the AERONET station. Level 1.5 data was used, because the majority of the station did not yet have level 2.0 data available. The results are plotted in Figures 11 and 12.

7.1.2.1 Comparison of AOT

The TROPOMI AOT measurements within 200 km and 15 minutes of the AERONET measurements were averaged to be compared to a single AERONET AOT measurement. The distance of a TROPOMI measurement to the AERONET station can be significant and introduces an uncertainty in the comparison, which is indicated by the horizontal error bar. Furthermore, in the averaging, the TROPOMI measurements were weighted by distance. TROPOMI performs many measurements during an overpass within 200 km of the AERONET station, and the spread of the averaged measurements is indicated by the vertical error bars.

In section 5.2 the requirements for the AOT were defined. The measurements that satisfy these requirements are those within the grey area in the scatterplots of Figures 11 and 12. The measurements that do not satisfy the requirements are indicated in blue in the figures. The fraction of measurements that are satisfy the requirements are listed table 1. Furthermore, in this table the slope and offset of a linear least squares fit to the measurements for each station is given.

The results show a reasonable comparison of TROPOMI AOT to AERONET AOT, with the majority of the measurements near the AERONET station satisfying the requirements. In most cases the fraction of measurements within the requirements is high and well above 0.5. Only in Tomsk station and Ilorin it is below 0.5. In both cases, the selection of the Weakly Absorbing (WA) aerosol model, which is the default, is the reason for the majority of the misfit of the measurements.

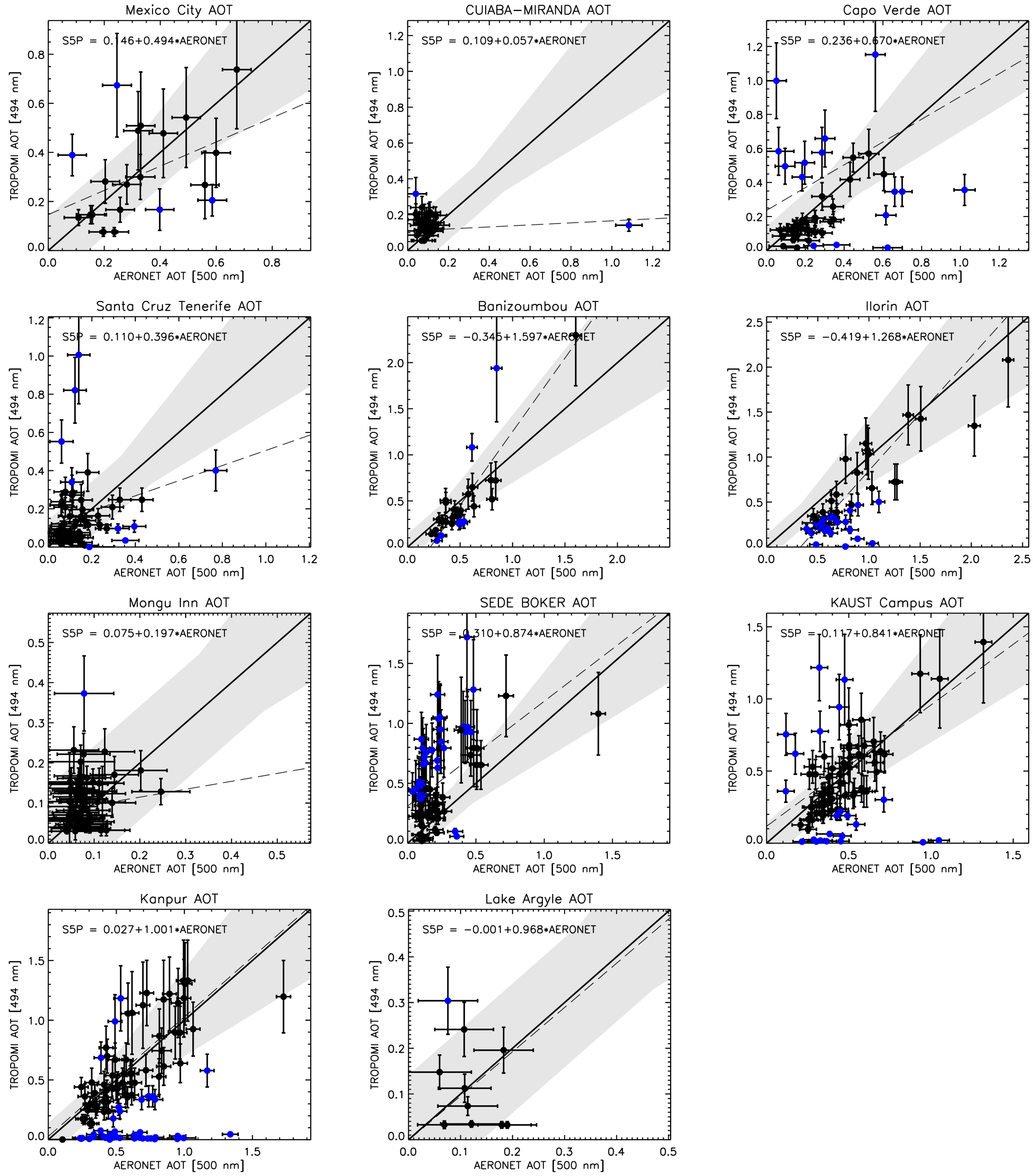

Figure 11: Scatterplots for all selected tropical AERONET stations. For each AERONET measurement (roughly every 15 minutes) the S5P AOT measurements within these 15 minutes closer than 200 km to the station were averaged, weighted by distance to the station. The spread of the averaged TROPOMI measurements within these 15 minutes is indicated by the vertical error bar, while the horizontal error bar indicates the relative average distance to the AERONET site. The uncertainty limits defined in section 5.2 are indicated by the grey area. Measurements that are not within the requirement limits are plotted in blue. The fraction of measurements that satisfy the requirements are listed in table 1. The dashed line indicates a linear least squares fit to the measurements. The fit parameters are indiced at the top of each plot, and listed in table 1.

7.1.2.2 Detailed comparision of AOT

Four of the AERONET station were used to investigate further results. The comparison with AERONET was repeated for these stations using half a year of TROPOMI AOT measurements around those stations, and the results of the AOT comparisons were related to the type selections, see Figure 13. For the stations Beijing and

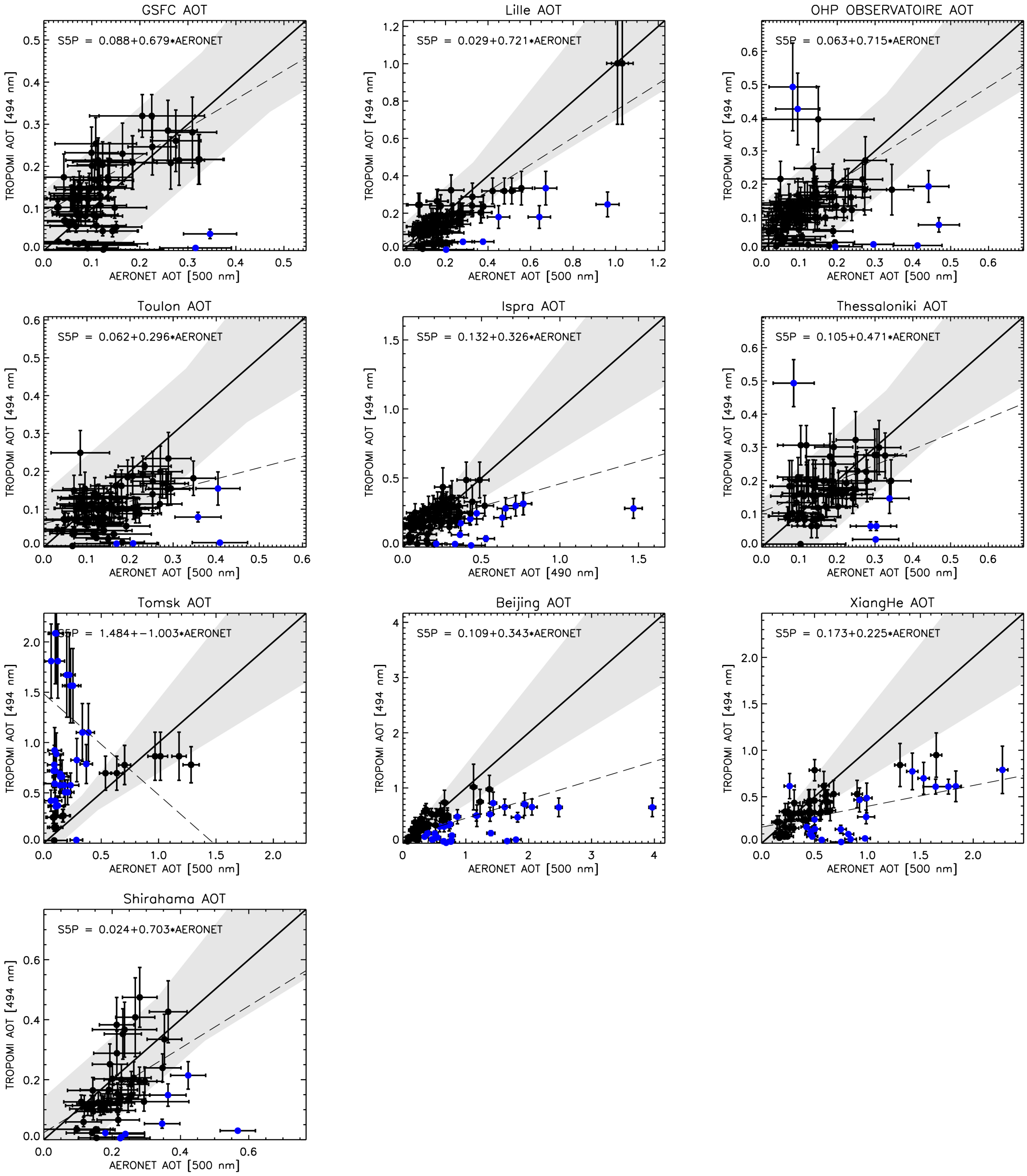

Figure 12: Scatterplots for all selected AERONET stations in the north temperate zone.

Kanpur the comparison with AERONET was poor. In Fig 13 the histograms show that around these stations the Weakly Absorbing (WA) aerosol type is almost exclusively selected, which is the default in the absence of desert dust or smoke. This works well over oceans, where the dominant aerosol type is sea salt, but over Beijing and Kanpur the dominant aerosol sources are anthropogenic, which increaslingly release absorbing aerosols. This is not reflected in the aerosol type selection, resulting in a mismatch in AOT. AOT from single view instruments is known to depend strongly on *a priori* assumptions [RD11, RD12].

For the stations Banizoumbou and Santa Cruz Tenerife, the comparisons are quite good. In these cases, the aerosol types are still dominated by weakly absorbing aerosols, but desert dust and, in the case of Banizoumbou, smoke also make up a large fraction of the selected aerosol types. Therefore, the AOT retrieval produces much better results. Tenerife, being an island, is dominated by sea salt. But during regular sand storms from the Sahara, the aerosol mixture will be strongly desert dust dominated. Banizoumbou is also prone to desert dust incursions and is also influenced by smoke from extensive vegatation fires, next to scattering

Table 1: Fit parameters of linear least squares fits in figures 11 and 12, and the percentage of AOT measurements that satisfy the requirements, and fit parameters of linear least squares fits in figures 14 and 15.

AERONET station	AOT fit		Fraction	SSA fit	
	offset	slope	within requirements	offset	slope
Mexico City	0.146	0.494	0.773	1.416	-0.455
CUIABA-MIRANDA	0.109	0.057	0.926	1.009	-0.010
Capo Verde	0.236	0.670	0.688	1.168	-0.223
Santa Cruz Tenerife	0.110	0.396	0.880	0.908	0.081
Banizoumbou	-0.345	1.597	0.724	2.042	-1.200
Ilorin	-0.419	1.268	0.452	1.542	-0.684
Mongu Inn	0.075	0.197	0.985	1.005	-0.022
SEDE BOKER	0.310	0.874	0.575	0.519	0.493
KAUST Campus	0.117	0.841	0.728	1.048	-0.075
Kanpur	0.027	1.001	0.598	1.543	-0.662
GSFC	0.088	0.679	0.975	1.008	-0.017
Lille	0.029	0.721	0.927	0.730	0.266
OHP OBSERVATOIRE	0.063	0.715	0.915	0.788	0.207
Toulon	0.062	0.296	0.943	1.237	-0.309
Ispra	0.132	0.326	0.828	0.878	0.117
Thessaloniki	0.105	0.471	0.903	0.446	0.562
Tomsk	1.484	-1.003	0.298	1.134	-0.190
Beijing	0.109	0.343	0.565	0.972	0.009
XiangHe	0.173	0.225	0.642	0.972	0.009
Shirahama	0.024	0.703	0.857	1.416	-0.455

aerosols from the ocean or industrial activity.

7.1.2.3 Comparison of SSA

Next, the single scattering retrieval by TROPOMI was compared to AERONET retrievals of single scattering albedo for the same stations as in the previous section. The inversion retrieval by AERONET is considered to be very reliable. Here, AERONET level 3, Version 1.5 was used, since level 2.0 data were not yet available.

In Figures 14 and 15 scatterplots are presented for TROPOMI SSA measurements within 200 km and 15 minutes of the AERONET measurements. The measurements were averaged to be compared to a single AERONET SSA measurement. The distance of a TROPOMI measurement to the AERONET station can be significant and introduces an uncertainty in the comparison, which is indicated by the horizontal error bar. Furthermore, in the averaging, the TROPOMI measurements were weighted by distance. TROPOMI performs many measurements during an overpass within 200 km of the AERONET station, and the spread of the averaged measurements is indicated by the vertical error bars.

Clearly, the comparison of TROPMI SSA with AERONET data is very poor. There is no correlation between these measurements. The main reason for these discrepancies is the known dependence of single view satellite retrievals on the (correct) choice of aerosol type in the algorithm. This affects the AOT retrieval, but even stronger derived products like SSA (and AAOT) [RD13, RD14].

7.1.3 Conclusion

The TROPOMI AOT at 494 nm shows a good correlation to AERONET AOT measurements at 500 nm for AERONET stations Lecce and Ispra. This was concluded on the basis of direct intercomparison between the two. Satterplots showed good agreement with differences no more than about 0.1 in AOT. A good temporal correlation was also found in both Jan–March 2019 and 2020.

A global comparison between thirty AERONET stations and TROPOMI AOT shows high correlation between measurements from both instruments in March and April 2021, with the majority of the AOT measurements being within the requirements. The selected AERONET stations were distributed such that all aerosol types were represented in the measurements. Measurements outside the requirements were often caused by a poor

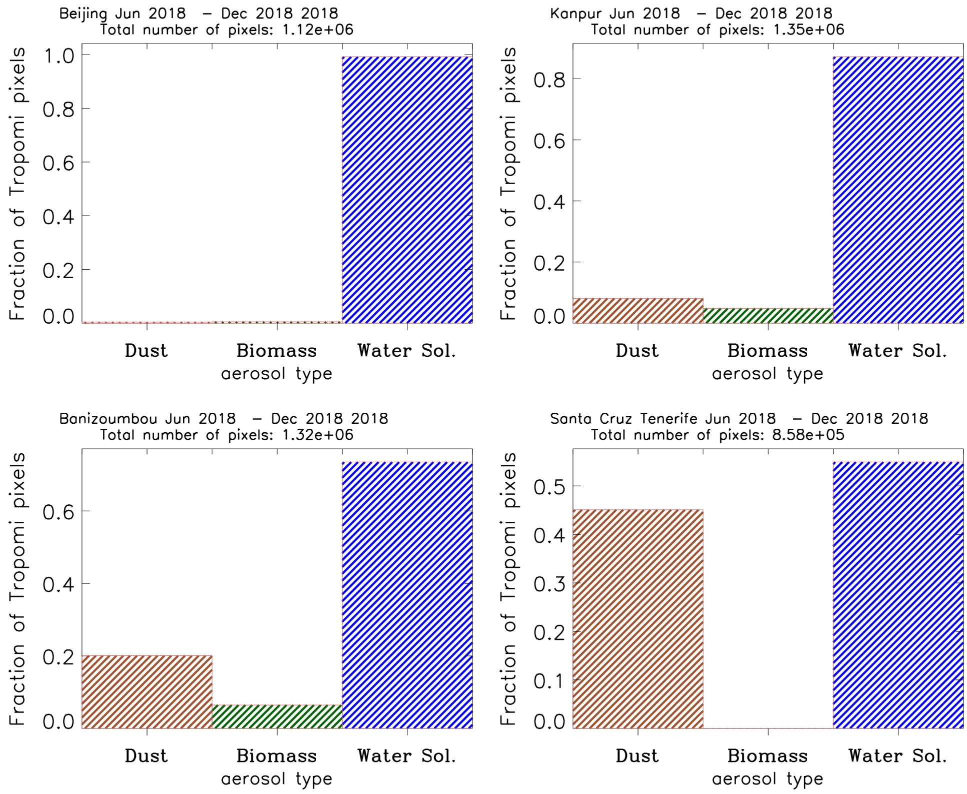

Figure 13: Type selection histograms for four stations in Figure 10.

aerosol type selection, which makes the fitting of aerosol intrinsic properties difficult, resulting in a mismatch in AOT. This was strongly dependent on the region that was studied.

For SSA the comparison with AERONET shows a very poor correlation. This is a know deficiency of current satellite SSA products, especially single-view instruments like TROPOMI. No skill can be expected from such instruments for SSA and AAOT. New, upcoming satellite missions, dedicated to aerosol retrievals, will bring spectral, polarised measurements at multiple angles, which are essential for the retrieval of intrinsic aerosol propoerties. Advanced algorithms, like GRASP, will benefit from this multitude of information and can be expected to derive much more accurate AOT and SSA products.

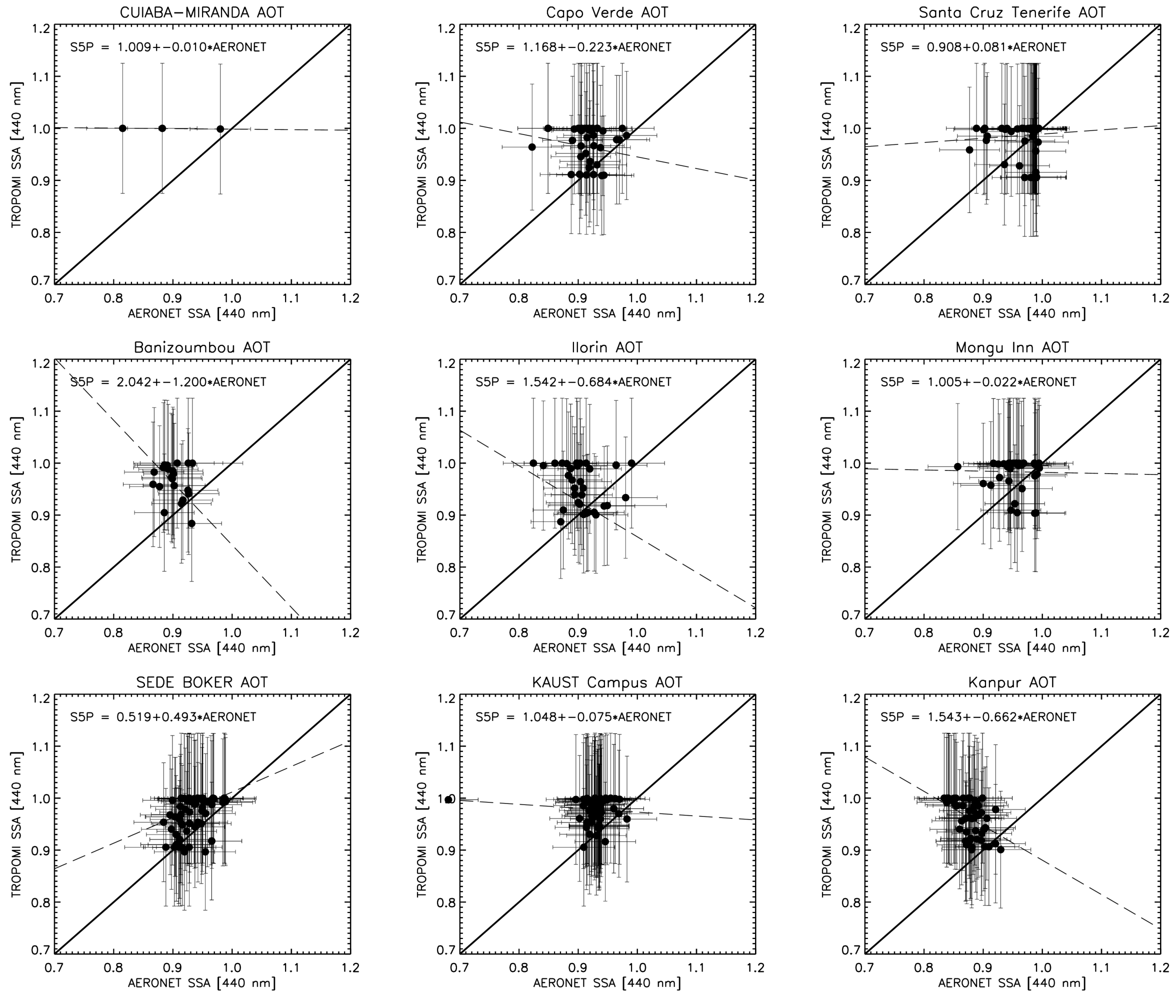

Figure 14: Scatterplots for all selected tropical AERONET stations. For each AERONET measurement (roughly every 15 minutes) the TROPOMI SSA measurements within these 15 minutes closer than 200 km to the station were averaged, weighted by distance to the station. The spread of the averaged TROPOMI measurements within these 15 minutes is indicated by the vertical error bar, while the horizontal error bar indicates the relative average distance to the AERONET site. The dashed line indicates a linear least squares fit to the measurements. The fit parameters are indiced at the top of each plot, and listed in table 1.

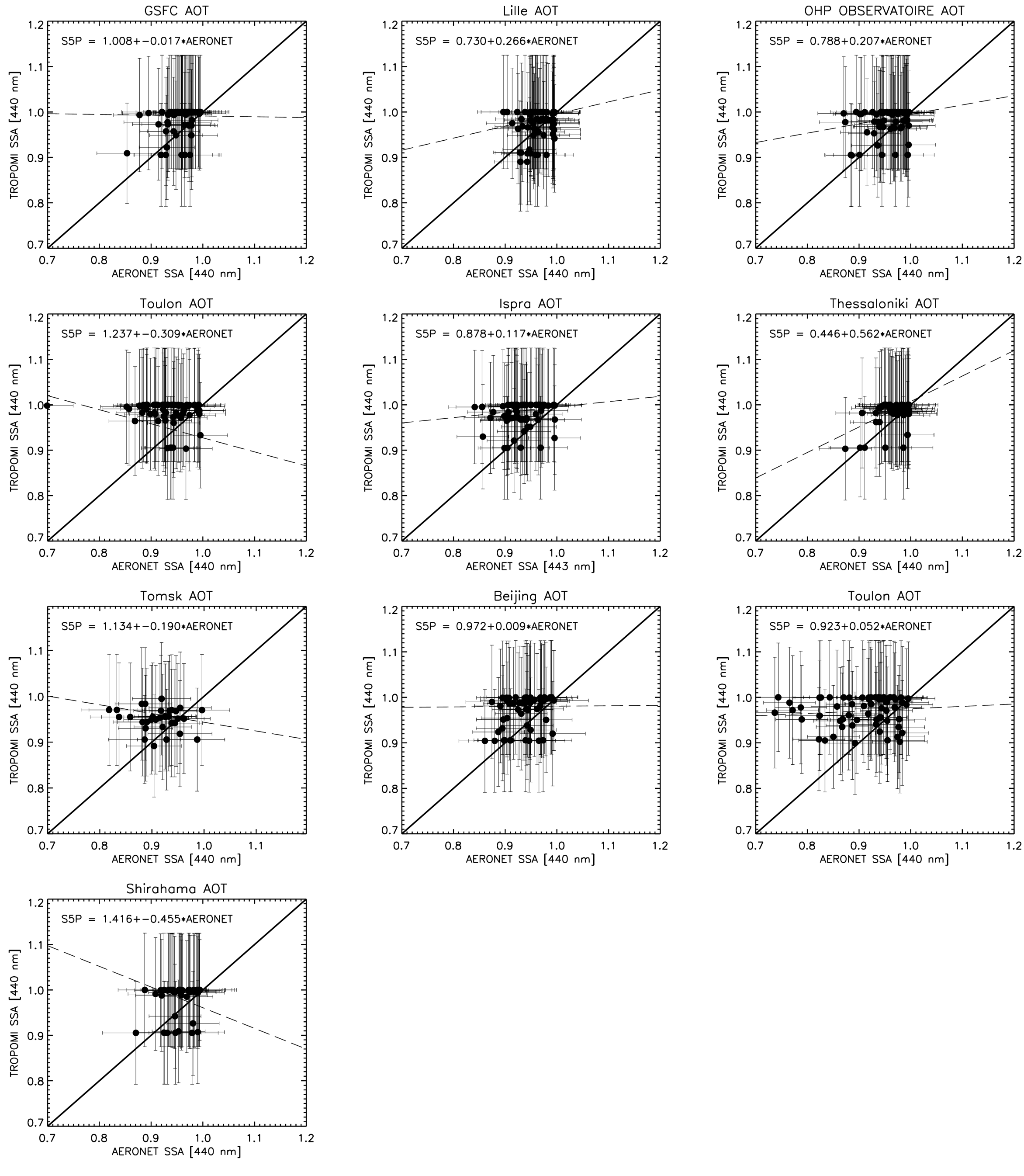

Figure 15: Scatterplots for all selected AERONET stations in the north temperate zone.

7.2 Global AOT compared to VIIRS data

Sentinel-5 flies in synchrony with Suomi-NPP, following it at about 5 minutes, which creates the opportunity to compare the products from instruments on both platforms. Here, the AOT from TROPOMI is compared to the Joint Polar Satellite System (JPSS) Risk Reduction Unique Aerosol Optical Depth product version 1.0 at 550 nm from Visible Infrared Imaging Radiometer Suite (VIIRS). VIIRS AOD is available on a fine grid of about 0.75 km^2 at nadir, in granules covering about 2.5 minutes. TROPOMI AOT is available on a much coarser grid of about 5.5 km along-track at nadir. Therefore, both products were regridded to a regular $0.5^\circ \times 0.5^\circ$ grid. Data from 1 August 2018 were used, when several aerosol events happened around the globe, most notably a desert dust outbreak over the tropical Atlantic Ocean and vegetation fires in Southern Africa and Siberia.

The regridded TROPOMI and VIIRS data are plotted in Figure 16. Nine regions were selected to directly compare the AOT from VIIRS and TROPOMI, as indicated in the figure. For each of the regions all the AOT measurements from both instruments were compared.

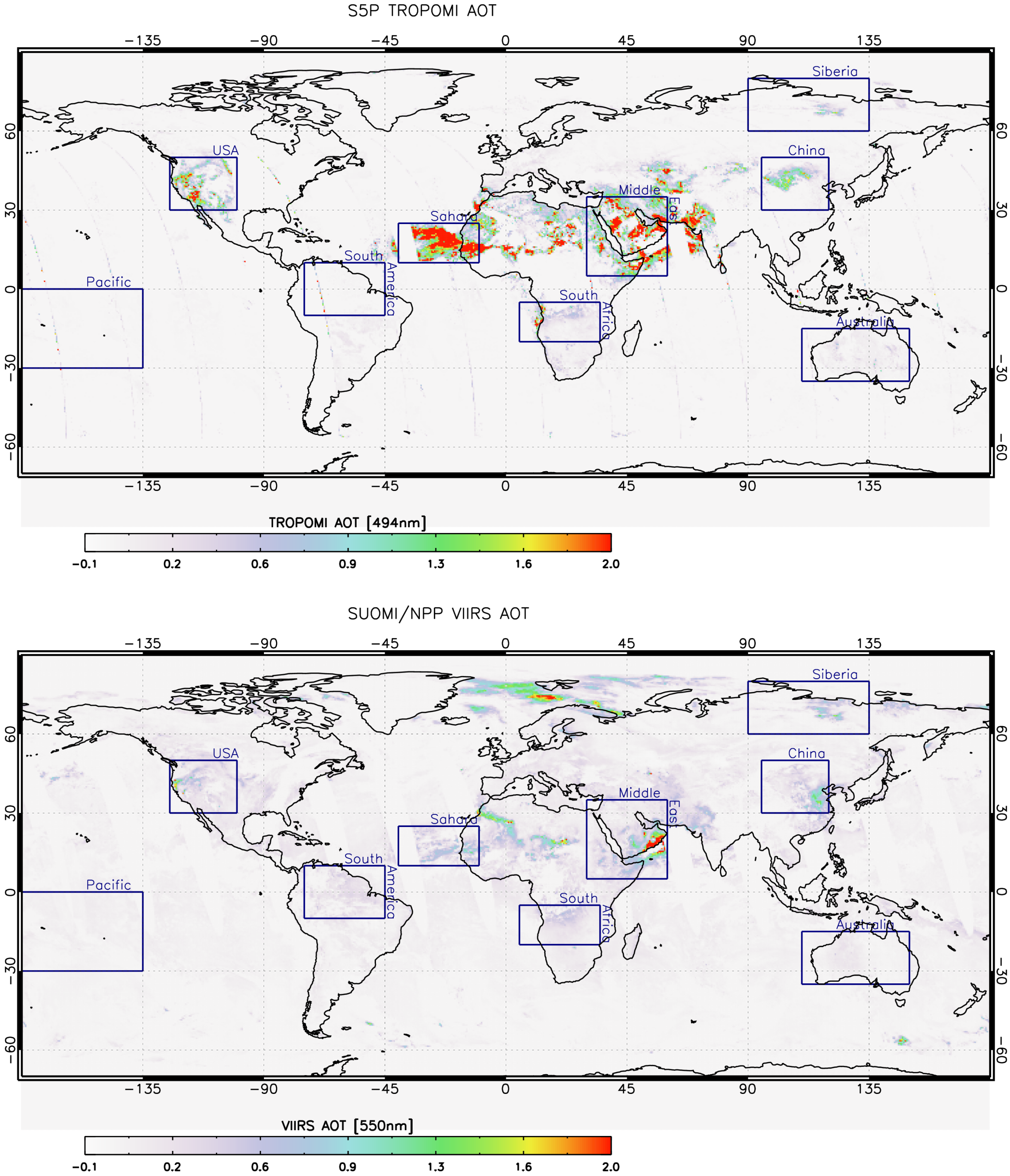

Figure 16: (top) TROPOMI AOT at 494 nm on 1 August 2018, regridded to a $0.5^\circ \times 0.5^\circ$ grid. (bottom) Regridded VIIRS AOD at 550 nm on 1 August 2018.

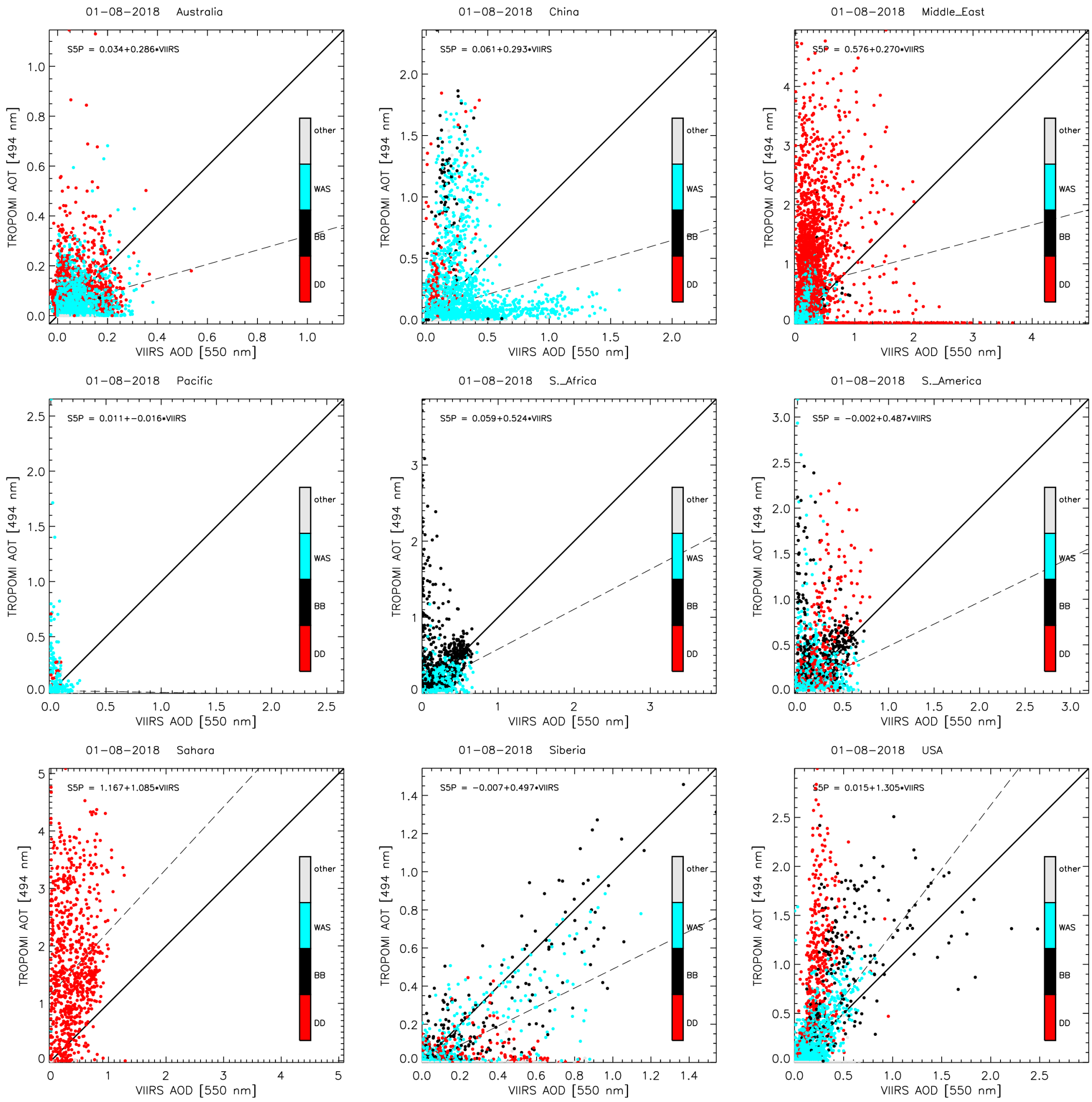

Figure 17: TROPOMI AOT at 494 nm versus VIIRS AOD at 550 nm at various locations on 1 August 2018. Colors refer to the selected aerosol type in the TROPOMI AOT retrieval. The dashed line shows the linear least squares fit to the measurements.

In Figure 17 the results are plotted of the VIIRS-TROPOMI AOT comparison for the selected regions in Figure 16. Clearly, the aerosol optical thickness from both instruments show little correlation. TROPOMI AOT is often much higher than that from VIIRS, which generally shows little variation. Especially for the desert dust type in Middle East Sahara and USA, the TROPOMI AOT is high, up to 4, where VIIRS OAD is usually below 1 or 2. The same is true for the smoke aerosol type in China and USA, TROPOMI showing a larger variation, where VIIRS is generally moderately low.

This correlation can be slightly improved by zooming in on obvious cases of high aerosol, but in general the products behave quite differently. Again, this is not uncommon. Both algorithms rely heavily on the selection of aerosol models in the retrievals. If this is different between the instruments, the results will differ.

8 Conclusion

The TROPOMI AOT and derived SSA products were validated using ground-based and satellite data. For the ground-based validation AERONET stations at varying locations around the globe were used, to ensure that all common types of aerosols were represented in the comparisons. TROPOMI AOT and SSA data from various sources and at different times were used. Some scientifically produced data were produced early in the development of the algorithm, to benefit from the lockdown regulations in early 2020 in Italy, which showed severe restrictions for industry and traffic, which was expected to be reflected in the aerosol distributions. Furthermore, data were processed on the newly developed PAL environment, which allows the algorithm developer to process data at an almost operational level. Two months worth of data from this platform were used to compare global data with AERONET stations. No differences were found between the PAL-produced product and the scientific data.

Comparisons of AOT from TROPOMI with AERONET data showed good comparisons, with the majority of the data being within the requirements. For most stations the fraction of data falling within the requirements was highre than 80%. For a few stations this dropped below 60% and one station had less than 30% TOA measurements within the requirements. The main reason for the lower correlations is the selection of aerosol type, for which the algorithm is very sensitive. With an inappropriate aerosol model the algorithm will not be able to retrieve an accurate AOT.

A comparison of AOT from TROPOMI with collocated VIIRS AOD measurements did not show a good correlation, even though S5P and Suomi-NPP fly in sychrony and the collocation is almost perfect. Both algorithms have their own aerosol model selection strategy, and this results in rather large differences between the products. The intrinsic properties of aerosols are important in the inversion schemes, and if one or either model is incorrect the retrieval will fail to give consistent results.

The previous problem is most palpable in the SSA comparison. No correlation was found between the SSA from TROPOMI compared to AERONET. Even though the AOT compared reasonably well, the SSA shows no skill. This is in accordance with other satellite SSA and AAOT products, which currently show no to very low skill. This problem should be resolved using satellite missions dedicated to retrievals of aerosol properties and algorithms that are able to utilize all the information in the measurements of these missions. Examples are upcoming satellite missions like 3MI and EarthCare, and algoriths like GRASP.